

Thickness-dependent thin-film resistivity: Application of quantitative scanning-tunneling-microscopy imaging

G. Reiss, E. Hastreiter, H. Brückl, and J. Vancea

Institut für Angewandte Physik III, Universität Regensburg, Universitätsstrasse 31, D-8400 Regensburg, Germany

(Received 5 November 1990)

The dependence of thin-film resistivity on the thickness is known to be strongly influenced by the interaction of the conduction electrons with the surface. Great efforts have been made in recent years, mainly concerning the quantum-mechanical description of the surface scattering. Detailed discussions of this problem, however, suffer from the lack of information concerning the real topography of thin-film surfaces. The development of scanning tunneling microscopy (STM) now gives the chance of direct, quantitative imaging. In this paper, we use the topographic information of STM to improve the fitting of theoretical descriptions to the measured thickness dependence of the resistivity. The transport parameters obtained from these calculations show a high degree of physical consistency.

INTRODUCTION

The thickness dependence of thin-film resistivity is the subject of extensive discussions in literature. Clearly, the surface gives rise to additional scattering of the conduction electrons (CE). This mechanism considerably enhances the resistivity, as long as the intrinsic scattering length (mean free path l_∞) is of the same order as the film thickness. The resistivity enhancement is thus a direct manifestation of the fundamental electronic transport parameter l_∞ . Quantitative descriptions of the resulting thickness dependence of the resistivity $\rho_{\text{film}}(d)$ (where d is the film thickness) have been given, for example, by Fuchs¹ within a semiclassical Boltzmann formalism. Recent works²⁻⁷ gave quantum-mechanical treatments of this phenomenon using first-order perturbational theories. In contrast with the semiclassical approach,¹ these calculations take into account the splitting of the electronic density of states (DOS). In the limit of continuous DOS, i.e., for $d \gg 2\pi/k_F$ (where k_F is the Fermi wave vector) the semiclassical as well as the quantum-mechanical treatment show a correction to the bulk resistivity ρ_∞ proportional to $1/d$, i.e.,

$$\rho_{\text{film}} = \rho_\infty \left[1 + f \left(\frac{1}{d}, c l_\infty \right) \right]. \quad (1)$$

The constant c is $(1-p)$ in the semiclassical treatment¹ (p is the specular parameter) or h^2 in the quantum-mechanical treatment of, for example, Tešanović and co-workers^{2,3} (h is the rms value of the microscopic roughness of the surface potential, which of course should not exceed the Fermi wavelength).

Experimentally, however, the situation for polycrystalline films is not as simple as has previously been assumed. A direct application of these theoretical approaches thus is not practicable: Usually, polycrystalline films exhibit both a microscopic (h) and a mesoscopic roughness (H). Whereas the lateral correlation length τ_h of the first one is of the order of 1 nm or below,^{4,6,8,9} τ_H coincides with the size of the islands (i.e., mesoscopic topographic features) found on thin-film surfaces. This is usually larger than at

least 10 nm;¹⁰ for polycrystalline films, τ_H corresponds to the mean crystallite size commonly ranging between 20 and 100 nm. Thus the microscopic roughness of the potential gives rise to surface scattering of the CE, which should be treated quantum mechanically. The mesoscopic roughness H , however, represents large-scale fluctuations of the local film thickness and can be taken into account by averaging the local resistivity [Eq. (1)] over the whole film:^{7,11-13}

$$\rho_{\text{film}} = \langle \rho_{\text{loc}} \rangle_{\text{film}}. \quad (2)$$

If the mean film thickness d_m approaches H , this gives rise to an additional correction of the resistivity which is of the order of $1/d^2$.

Although good agreement can be obtained by fitting the theory to experimental ρ_{film} -vs- d_m curves for single films^{14,15} as well as for multilayered structures,¹⁶ the reliability of the obtained parameters is still under discussion. This is mainly due to the lack of knowledge concerning the detailed shape of the surface topography; in Ref. 11, for example, the mesoscopic roughness was described by a simple sinusoidal dependence, i.e., by one parameter representing the amplitude. Clearly, the results of quantitative STM imaging can remove this oversimplification. In this paper, we discuss the reliability of this new application of STM, using the example of thin polycrystalline Ni films.

EXPERIMENT

The films have been evaporated in UHV with 0.1 nm/sec onto fire-polished Corning glass. In order to obtain stable films at room temperature, the substrates were held at 430 K and immediately cooled down to 300 K after the evaporation. Details of the film production can be found, for example, in Refs. 12 and 15, and the references therein. The resistivity was measured using a conventional four-probe technique.¹² The structural characterization of the films were performed *ex situ* mainly with STM as well as with transmission electron microscopy (TEM) and Auger electron spectroscopy (AES). A detailed description of our STM can be found in Ref. 10.

RESULTS AND DISCUSSION

STM

For a quantitative interpretation of the thickness-dependent resistivity of polycrystalline thin films, STM first has to clear up the dependence of the surface's structure of the film thickness. Therefore, investigations have been performed at different stages of the film growth. Two typical examples for our Ni films with thicknesses of 10 and 20 nm are shown in Figs. 1(a) and 1(b), respectively.

Using a formalism reported recently,^{17,18} we conclude that both images are highly resolved, i.e., more than 97% of the real surface can be imaged by the tunneling tip. This must be regarded as a precondition for a reliable quantitative analysis. Qualitatively, both images show strongly corrugated but similar surfaces; this statement, however, is not sufficient for an introduction of STM results into quantitative theories. In Ref. 19, we therefore proposed a quite complete characterization of the mesoscopic surface roughness:

(a) Figure 2 shows the height distributions $r(H)dH$ of the two STM images of Fig. 1; $r(H)dH$ is the relative part of the surface located between height H and $H+dH$. Here, $H=0$ when the height axis equals the mean film thickness d_m .¹⁹ Given reasonable resolution, this function gives a good estimate of the roughness. As can be seen

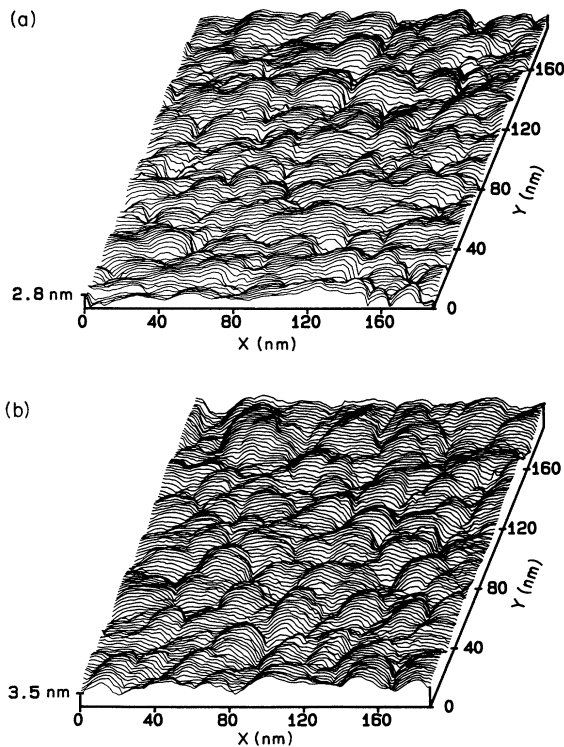


FIG. 1. (a) Scanning tunneling microscopy image of a 10-nm-thick Ni film on glass substrates evaporated in UHV at 430 K (raw data). (b) STM image of a 20-nm-thick Ni film prepared under the same conditions as the film in (a) (raw data).

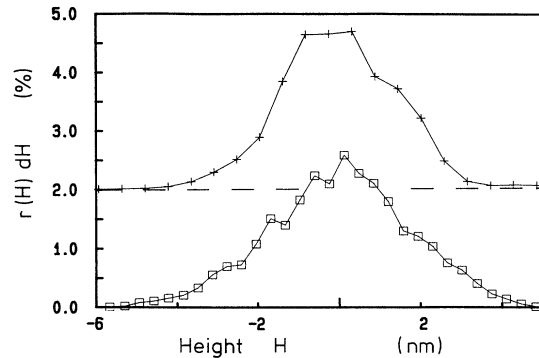


FIG. 2. The roughness distribution $r(H)dH$ of the two films of Fig. 1. Crosses: thickness 10 nm; squares: thickness 20 nm. The curve of the 10-nm-thick films is shifted by 2%.

from Fig. 2, the roughness distribution remains quantitatively the same for the two Ni thicknesses (10 and 20 nm). The halfwidth of both curves amounts to (3.0 ± 0.2) nm, the maximum depth of the surface irregularities is 6 nm below d_m , and the height of the islands is smaller than 5 nm. Thus, as demonstrated by this STM result, the roughness of the continuous Ni films under discussion does not change with thickness, at least in the range $10 \text{ nm} < d_m < 20 \text{ nm}$.

(b) The second task of STM imaging is the characterization of the lateral extensions of the surface corrugations. For this purpose, the autocorrelation function $f_{ac}(\tau)$ gives a good estimate of the mean island (i.e., crystallite) sizes.¹⁹ In Fig. 3, we show $f_{ac}(\tau)$ obtained from the two films of Fig. 1.

Superimposed on the usual exponential behavior, both autocorrelations show at least two additional features for $\tau > 0$; the distance is (30 ± 2) nm in both cases (see Fig. 3). This indicates a well-defined distribution of island sizes (i.e., the distribution does not follow a white-noise law). Thus the mean island sizes can be estimated to be between 28 and 32 nm for $d_{Ni}=10$ nm as well as for $d_{Ni}=20$ nm.

In summary, the STM analysis yields constant values for the roughness as well as for the correlation lengths in

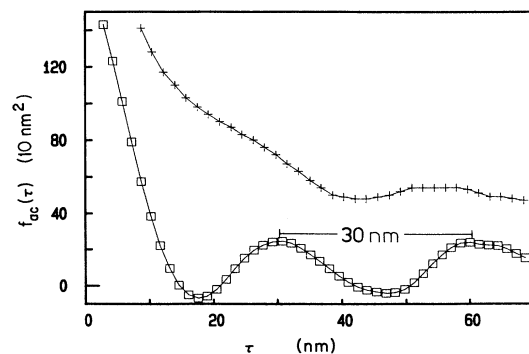


FIG. 3. Autocorrelation functions $f_{ac}(\tau)$ for the two films of Fig. 1. Crosses: thickness 10 nm; squares: thickness 20 nm. The mean distance between the two maxima (30 nm) is indicated.

the thickness range between 10 and 20 nm. The next task is the introduction of the results discussed in this paragraph into quantitative theories of the thickness-dependent resistivity.

STM results and the thin-film resistivity

Theories dealing with thickness-dependent resistivity^{1-7,11} commonly make use of three parameters. In a combination of the model of Tešanović and co-workers,^{2,3} with an estimate of an averaged resistivity,^{7,11,13} these are: ρ_∞ —the resistivity of infinitely thick (i.e., bulk) material, $l_\infty h^2$ —the product of the intrinsic mean free path and the square of the microroughness of the surface potential, and $H(x)$ —a one-dimensional function describing the mesoscopic surface roughness, i.e., the fluctuating film thickness.

For the films described in the foregoing section, the function $H(x)$ can be replaced by the results of quantitative STM analysis. Two important preconditions, however, must be satisfied. The first is that the correlation length τ_H must be much larger than the Fermi wavelength λ_F ; this is fulfilled for our films. The second is that the mean height $\langle H \rangle$ of the surface corrugations must be much smaller than the corrugation length τ_H .⁷ With the data obtained for our films, a ratio of $\langle H \rangle / \tau_H < 0.13$ can be estimated.

Therefore, the STM results can be used for the construction of $H(x)$. The STM analysis, however, yields $r(H)dH$, representing the two-dimensional distribution of roughnesses, whereas $H(x)$ is a one-dimensional height function. In order to evaluate $H(x)$ from $r(H)dH$, we state that this height function should correctly represent the real surface, i.e., $H(x)$ must give the same height distribution as the original STM image.

From this statement, the equation

$$r(H_0)dH = \frac{dH}{dH/dx|_{H(x)=H_0}} \quad (3)$$

can be found. Figure 4 shows the result of the evaluation of Eq. (3), i.e., the one-dimensional height function $H(x)$ corresponding to the STM images of Fig. 1. This function now will be introduced into the averaging procedure [Eq. (2)] of the thin-film resistivity.

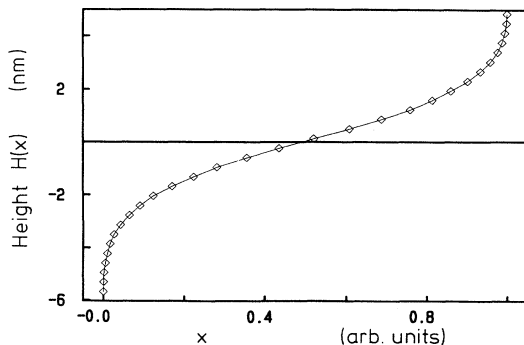


FIG. 4. The one-dimensional height function $H(x)$ for our Ni films evaluated from the roughness distribution of Fig. 2.

The thickness-dependent resistivity

For the quantitative description of the thickness-dependent resistivity, the model of Tešanović and co-workers^{2,3} gives the local values of ρ_{film} :

$$\rho_{\text{loc}}[d(x), l_\infty h^2, \rho_\infty] = n_c \rho_\infty \left\{ \sum_{n=1}^{n_c} \left[1 + \frac{(l_\infty h^2) k_F^2}{6\pi d(x)} \left(\frac{n}{n_c} \right)^2 \right]^{-1} \right\}^{-1} \quad (4)$$

Here, n_c is the number of occupied subbands and $d(x)$ is the local film thickness. In our discussion, $d(x)$ is given by

$$d(x) = d_m + H(x) \quad (5)$$

Here, $H(x)$ is the height function of the roughness obtained from STM results [see Eq. (3) and Fig. 4].

The averaged, i.e., measured resistivity then becomes¹¹

$$\rho_{\text{film}}(d_m, l_\infty h^2, \rho_\infty) = \frac{d_m \rho_\infty}{l} \int_0^l \frac{\rho_{\text{loc}}[d(x), l_\infty h^2, \rho_\infty]}{\rho_\infty d(x)} dx \quad (6)$$

With this description, the experimental results can be fitted by a variation of only two parameters, i.e., ρ_∞ and the product $l_\infty h^2$.

The results of this procedure are shown in Fig. 5 for the Ni film presented in the STM image of Fig. 1(b). There is good agreement between the theoretical and the experimental curve for Ni thicknesses larger than about 7 nm. From the STM results of Fig. 2, we can conclude that our films become continuous at a thickness of about 6 nm. Thus a percolative behavior, following a scaling law rather than the theory discussed above, can be expected below this thickness. Above this critical value of d_m , the experiment can be fitted within less than 3% by the theoretical expressions of Eqs. (4)–(6). The parameters obtained from the fitting calculations are $\rho_\infty = (19.5 \pm 0.5) \mu\Omega \text{ cm}$

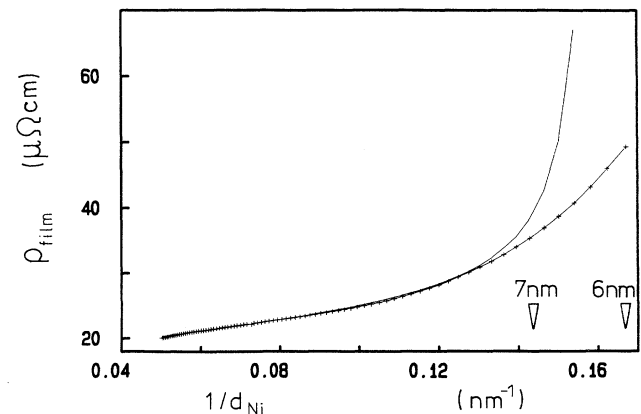


FIG. 5. The resistivity ρ_{film} as a function of the inverse film thickness of the Ni film of Fig. 1(b) measured during evaporation (curve containing the data points) and the fitted theory (solid line). Parameters: $\rho_\infty = 19.5 \mu\Omega \text{ cm}$, $l_\infty h^2 = 1.25 \text{ nm}^3$. The critical values of the roughness found by STM are indicated.

and $l_{\infty}h^2 = (1.25 \pm 0.1) \text{ nm}^3$. The corresponding values of the single-crystalline material are $\rho_{SC} = 7 \mu\Omega \text{ cm}$ and $l_{SC} \approx 17 \text{ nm}$.^{20,21}

Whereas the obtained values are numerically stable within a few percent due to fitting a nonlinear curve by only two parameters, their physical consistency should be checked. The onset of the Ohmic conductivity is located at $d_{on} \approx 3.5 \text{ nm}$, i.e., just at the value of the mean roughness found by STM (see Fig. 2). This value naturally should mark the beginning of the percolation mechanism between 3.5 and 7 nm. At thicknesses exceeding the maximum depth of the bumps in the surface, i.e., for really continuous films, the experimental curve closely follows the theoretical descriptions of Eqs. (4)–(6). The value of ρ_{∞} can be determined very accurately by measuring the resistivity of thick films. We found, for example, $\rho_{\infty} = (19 \pm 1) \mu\Omega \text{ cm}$ for 100-nm-thick films grown under identical conditions. The product $l_{\infty}h^2$ has to be physically consistent. In particular, h must be smaller than the Fermi wavelength. Assuming that the increase of the resistivity is due only to statistical (i.e., Boltzmann) scattering, the minimal value of l_{∞} can be estimated from

$$l_{\infty} > l_{SC} \frac{\rho_{SC}}{\rho_{\infty}}. \quad (7)$$

On the other hand, $l_{\infty} < l_{SC}$ must be fulfilled, anyway. Thus, $6 \text{ nm} < l_{\infty} < 17 \text{ nm}$ can be evaluated from the fitting results. With $l_{\infty}h^2 \approx 1.25 \text{ nm}^3$, the possible range of the microscopic roughness of the surface potential will be $0.27 \text{ nm} < h < 0.45 \text{ nm}$.^{2,3} These values of h are plausible, especially below the Fermi wavelength λ_F . Note that no restriction for the parameters was introduced during the fitting calculation. The obtained parameters thus have a good physical consistency. Comparing the results with the original model of Fuchs,¹ a rather low specularity parameter ranging between 0.1 and 0.4 can be estimated²² from the results discussed above.

CONCLUSIONS

In summary, we applied the results of a quantitative STM analysis in order to obtain a realistic description of electronic dc transport in thin polycrystalline films, including the mesoscopic surface roughness. Provided reasonable resolution can be achieved, the height distributions and lateral correlation lengths of the surface topographies can be calculated from as-measured STM images. Due to their large correlation length, the evaluated distribution of the mesoscopic (i.e., nanometer-range) roughness can be introduced into the theoretical description of the thin-film resistivity by averaging the local resistivities. This procedure thus replaces one parameter of the theoretical description by quantitative experimental results.

Fitting the theoretical expressions to the experimental curves therefore can be performed by a variation of only two parameters: The bulk resistivity and the product of the intrinsic mean free path and the square of the microscopic roughness of the surface potential. The values resulting from this calculation show a high degree of physical consistency. As checked by STM results, the agreement between the experimental and theoretical curve becomes very good for continuous films. The obtained bulk resistivity agrees with the values measured on thick films. Additionally, the product $l_{\infty}h^2$ agrees with the theoretical expectations; especially, h turns out to be smaller than the Fermi wavelength.

Thus the results obtained so far seem to be very encouraging. Further efforts concerning two-dimensional calculations and a detailed evaluation of surface scattering due to the microscopic roughness are in progress.²³

ACKNOWLEDGMENTS

We would like to thank H. Hoffmann for his support of this work and F. Schneider for STM software.

¹K. Fuchs, Proc. Cambridge Philos. Soc. **34**, 100 (1938).

²Z. Tešanović, M. V. Jarić, and S. Maekawa, Phys. Rev. Lett. **57**, 2760 (1986).

³Z. Tešanović, J. Phys. C **20**, L829 (1987).

⁴G. Fishman and D. Calecki, Phys. Rev. Lett. **62**, 1302 (1989).

⁵D. Calecki and G. Fishman, Surf. Sci. **229**, 110 (1990).

⁶C. S. Chu and R. S. Sorbello, Phys. Rev. B **38**, 7260 (1988).

⁷N. Trivedi and N. W. Ashcroft, Phys. Rev. B **38**, 12298 (1988).

⁸J. M. Phillips, J. L. Batstone, J. C. Hensel, and M. Cerullo, Appl. Phys. Lett. **51**, 1895 (1987); see also Ref. 4.

⁹J. C. Hensel, R. T. Tung, J. M. Poate, and J. C. Unterwald, Phys. Rev. Lett. **54**, 1840 (1985); see also Ref. 6.

¹⁰J. Vancea, G. Reiss, F. Schneider, K. Bauer, and H. Hoffmann, Surf. Sci. **218**, 108 (1989).

¹¹Y. Namba, Jpn. J. Appl. Phys. **9**, 1326 (1970).

¹²J. Vancea, G. Reiss, and H. Hoffmann, Phys. Rev. B **35**, 6435 (1987).

¹³U. Jacob, J. Vancea, and H. Hoffmann, Phys. Rev. B **41**,

11852 (1990).

¹⁴J. Vancea, G. Reiss, and H. Hoffmann, J. Mater. Sci. Lett. **6**, 985 (1987).

¹⁵J. Vancea, Int. J. Mod. Phys. B **3**, 1455 (1989).

¹⁶G. Reiss, K. Kapfberger, G. Meier, J. Vancea, and H. Hoffmann, J. Phys. Condens. Matter **1**, 1275 (1989).

¹⁷G. Reiss, J. Vancea, H. Wittmann, J. Zweck, and H. Hoffmann, J. Appl. Phys. **67**, 1156 (1990).

¹⁸G. Reiss, F. Schneider, J. Vancea, and H. Hoffmann, Appl. Phys. Lett. **57**, 867 (1990).

¹⁹G. Reiss, H. Brückl, J. Vancea, R. Lecheler, and H. Hasreiter, J. Appl. Phys. (to be published).

²⁰G. T. Meaden, *Electrical Resistance of Metals* (Heywood, London, 1965).

²¹J. Callaway, Phys. Rev. B **7**, 1096 (1973).

²²U. Jacob, Ph.D. thesis, University of Regensburg, 1988 (unpublished). See also Ref. 13.

²³H. Brückl and G. Reiss (unpublished).